

Fake Nodes approximation for Magnetic Particle Imaging

Stefano De Marchi
Dip. di Matematica “Tullio Levi-Civita”
Università di Padova
 Padova, Italy
 demarchi@math.unipd.it

Wolfgang Erb
Dip. di Matematica “Tullio Levi-Civita”
Università di Padova
 Padova, Italy
 wolfgang.erb@lissajous.it

Elisa Francomano
Department of Engineering
Università di Palermo
 Palermo, Italy
 elisa.francomano@unipa.it

Francesco Marchetti
Dip. di Salute della Donna e del Bambino
Università di Padova
 Padova, Italy
 francesco.marchetti.1@phd.unipd.it

Emma Perracchione
Dip. di Matematica DIMA
Università di Genova
 Genova, Italy
 perracchione@dima.unige.it

Davide Poggiali
PNC - Padova Neuroscience Center
Università di Padova
 Padova, Italy
 poggiali.davide@gmail.com

Abstract—Accurately reconstructing functions with discontinuities is the key tool in many bio-imaging applications as, for instance, in Magnetic Particle Imaging (MPI). In this paper, we apply a method for scattered data interpolation, named *mapped bases* or *Fake Nodes* approach, which incorporates discontinuities via a suitable *mapping* function. This technique naturally mitigates the Gibbs phenomenon, as numerical evidence for reconstructing MPI images confirms.

Index Terms—Magnetic Particle Imaging, interpolation, radial basis functions, kernels

I. INTRODUCTION

Magnetic Particle Imaging (MPI) is a tracer-based tomographic technique of recent development that uses dynamic magnetic fields to provide *in vivo* functional images in a less invasive way compared to nuclear imaging, with high resolution and short acquisition time. MPI systems detect the spatial distribution of superparamagnetic nanoparticle tracers injected in the body, which are then naturally expelled by the animal body.

Image acquisition in MPI is performed by generating magnetic Field Free Point (FFP), which moves along a chosen sampling trajectory and induces a measurable voltage signal in a receive coil. The scattered data obtained from this signal acquisition process can then be interpolated and evaluated over a regular grid in order to obtain a human readable image. However such approximation may result inaccurate when dealing with highly varying signals, due to the well-known Gibbs effect [3], [20]. In this work we consider the so-called Fake Nodes approach [15] in order to deal with the artifacts caused by the Gibbs phenomenon, providing a stable and reliable approximation. We compare the results with other standard approximation techniques.

II. MAGNETIC PARTICLE IMAGING

Commonly used trajectories in MPI are Lissajous curves and thus we will use samples along Lissajous trajectories as approximation nodes.

A. Sampling on Lissajous nodes

For a vector of relatively prime numbers $\mathbf{n} = (n_1, n_2) \in \mathbb{N}^2$ and $\epsilon \in \{1, 2\}$, the Lissajous nodes are generated by equidistant samples along the curves

$$\gamma_\epsilon^{(\mathbf{n})}(t) = \left(\cos(n_2 t), \cos\left(n_1 t - \frac{\epsilon-1}{2n_2} \pi\right) \right). \quad (1)$$

These 2π -periodic Lissajous curves are the superposition of two perpendicular harmonic motions in the square $[-1, 1]^2$. For $\epsilon = 1$, the curve $\gamma_1^{(\mathbf{n})}(t)$ is degenerate, i.e. traversed twice as t varies from 0 to 2π , and is coincident to the generating curve of the Padua points [5], [6], [16] if $\mathbf{n} = (n, n+1)$. For $\epsilon = 2$, the curve $\gamma_2^{(\mathbf{n})}(t)$ is non-degenerate and is a typical sampling trajectory used in magnetic particle imaging, see [17], [22], [23]. Based on the curves $\gamma_\epsilon^{(\mathbf{n})}$ as generating trajectories, the Lissajous nodes are defined as the equidistant samples

$$\mathbf{LS}_\epsilon^{(\mathbf{n})} = \left\{ \gamma_\epsilon^{(\mathbf{n})} \left(\frac{\pi k}{\epsilon n_1 n_2} \right), \quad k = 0, \dots, 2\epsilon n_1 n_2 - 1 \right\}, \quad (2)$$

whose cardinality is

$$\#\mathbf{LS}_\epsilon^{(\mathbf{n})} = \frac{(\epsilon n_1 + 1)(\epsilon n_2 + 1) - (\epsilon - 1)}{2}.$$

In the upcoming experiments, we will use the nodes $\mathbf{LS}_2^{(33,32)}$ as reference interpolation nodes. These node sets were as well used in [11]–[13], [17], [22] for applications in magnetic particle imaging. A more accurate description of the data set is given in what follows.

B. Simulated dataset

As test data, we consider simulated MPI-measurements on a virtual phantom consisting of ferromagnetic particles aggregated in the form of two diagonal bars and discretized on an equidistant 201×201 grid in the square $[-1, 1]^2$. To obtain the MPI voltage signal we apply a measured MPI-system

matrix from [22] to this phantom. Based on the description given in [22], a reduced reconstruction is first performed on the Lissajous nodes. A full reconstruction is then obtained by the application of proper approximation methods as considered in this work. From now on we will refer to **reconstruction** when dealing with the process of approximating the full image from Lissajous samples.

III. MULTIVARIATE APPROXIMATION

Multivariate approximation (see e.g. [10]) is one of the most investigated topics in applied mathematics and finds applications in a wide variety of fields, such as in MPI. In what follows, we introduce the basic theory of approximation schemes and we remark that it fits many successful methods, such as multivariate splines, meshfree or meshless approaches and polynomial least squares. Then, we also introduce the approach based on mapped bases or Fake Nodes.

A. Approximation methods

Given $N + 1$ d -dimensional samples, $N, d \in \mathbb{N}$

$$\{(\mathbf{x}_i, y_i) \text{ s.t. } \mathbf{x}_i \in \Omega \subseteq \mathbb{R}^d, y_i \in \mathbb{R}\}_{i=0, \dots, N},$$

and a set of $M + 1$ basis functions ($M \leq N$)

$$\mathcal{B} = \{b_i : \Omega \subseteq \mathbb{R}^d \longrightarrow \mathbb{R}\}_{i=0, \dots, M},$$

the process of finding a set of real-valued parameters $\{c_i\}_{i=0, \dots, M}$ so that for $M = N$ the **interpolant**

$$\mathcal{P}_M(\mathbf{x}) = \sum_{i=0}^M c_i b_i(\mathbf{x}),$$

satisfies

$$\mathcal{P}_M(\mathbf{x}_i) = y_i \quad \forall i = 0, \dots, N, \quad (3)$$

is called scattered data **interpolation**.

If $M < N$ we refer to **least-squares** methods and \mathcal{P}_M is called **approximant**. Furthermore, the condition (3) is replaced by the following minimization problem

$$\min_{c_0, \dots, c_M} \sum_{i=0}^N |\mathcal{P}_M(\mathbf{x}_i) - y_i|^2. \quad (4)$$

We now drive our attention towards the Fake Nodes approach.

B. The Fake Nodes approach

The Fake Nodes approach, introduced in [15] consists in mapping the nodes with a properly chosen function

$$S : \Omega \longrightarrow \Omega' \subseteq \mathbb{R}^d$$

and computing the interpolant over the mapped nodes $\{S(\mathbf{x}_i)\}_{i=0, \dots, N}$ (or Fake Nodes from now on). For $\mathbf{x} \in \Omega$, the interpolant (or approximant) is given by

$$\mathcal{P}_M^S(\mathbf{x}) := \mathcal{P}_M(S(\mathbf{x})) = \sum_{i=0}^M c_i b_i(S(\mathbf{x})),$$

which satisfies the condition (3) or (4) in case of interpolation or least-squares approximation, respectively.

This approach is equivalent to using the **mapped basis**

$$\mathcal{B}^S = \{b_i \circ S : \Omega' \subseteq \mathbb{R}^d \longrightarrow \mathbb{R}\}_{i=0, \dots, M},$$

in the classical interpolation setting.

It has been shown in [15] that the Fake Nodes interpolation allows in many cases to choose a better node set for the given basis or for the given problem without the need of getting new samples from another set of nodes, as for instance in [4]. Numerical experiments shown in the next section support our claims.

IV. NUMERICAL EXPERIMENTS

We will now treat the 2-dimensional case of the MPI image reconstruction, using a piecewise linear mapping function and two different interpolation methods: least-squares 2D polynomial approximation and Radial Basis Function (RBF) interpolation.

A. Choice of the mapping function

Given the presence of different objects in the image, its interpolation is naturally affected by the Gibbs effect because of the step in signal intensity along the objects borders. A suitable mapping function for enhancing the reconstruction can be defined as follows.

Consider a bounded and compact image domain Ω . We now identify the objects in the image by segmentation, i.e. by finding subsets Γ_k such that

$$\Omega = \bigcup_{k=1}^m \Gamma_k \quad \text{and} \quad \Gamma_i \cap \Gamma_j = \emptyset \quad \forall i, j = 1, \dots, m,$$

then we can define the piecewise linear mapping function

$$S(\mathbf{x}) = \mathbf{x} + \sum_{k=1}^m \alpha_k \chi_{\Gamma_k}(\mathbf{x}),$$

where χ is the characteristic function and $\alpha_k = (ka, ka)$ a vector, where the chosen parameter $a \in \mathbb{R}$ has to be large enough to ensure non-overlapping of the Fake Nodes, for instance:

$$a > \text{diam}(\Omega) := \sup_{\mathbf{x}, \mathbf{y} \in \Omega} \|\mathbf{x} - \mathbf{y}\|.$$

The sets Γ_k have been estimated by segmentation, using the technique described in [13], [24].

In our setting the domain is $\Omega = [-1, 1]^2$. The parameter a is fixed as 2.01. We observed numerically that the reconstruction is not sensitive to particular choices of a , provided that a is *large enough*, as shown also in [15].

In Figure 1 we show the original node set (we fix $\mathbf{LS}_2^{(32,33)}$) and the Fake Nodes used in incoming experiments.

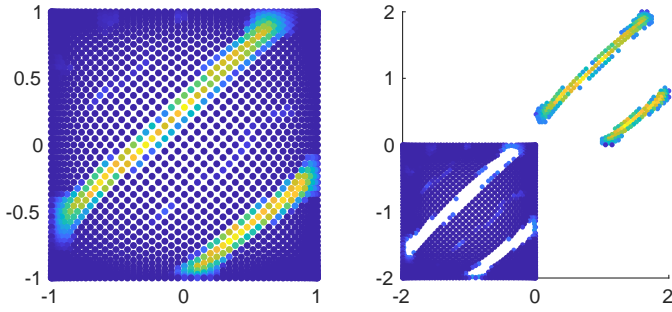


Fig. 1. Left: original nodes colored accordingly to the signal intensity. Right Fake Nodes obtained with the map S and $a = 2.01$ (right) colored accordingly to the signal intensity. The two objects were both considered in the same region and separated from the background.

B. Fake Nodes Polynomial Interpolation

The basis for the 2D polynomials of total degree K can be written as

$$\mathcal{B} = \left\{ x_1^i x_2^j \mid i, j = 0, \dots, K \text{ s.t. } i + j \leq K \right\}.$$

For the least squares approximation we fix $K = 21$.

C. Fake Nodes RBF Interpolation

We also perform experiments using RBFs. The basis for this method can be written as

$$\mathcal{B} = \{K(\cdot, \mathbf{x}_i)\}_{i=0, \dots, N}.$$

being $K(\cdot, \mathbf{x}_i) = \varphi(\|\cdot - \mathbf{x}_i\|_2)$ a kernel on $\Omega \times \Omega$, generated by a univariate radial real-valued function $\varphi(r)$, where r denotes the Euclidean distance. For this experiment we choose the Matérn functions of different regularities:

- $\varphi_0(r) = \exp(-r) \in C^0$
- $\varphi_2(r) = \exp(-r)(1 + r) \in C^2$
- $\varphi_4(r) = \exp(-r)(3 + 3r + r^2) \in C^4$
- $\varphi_6(r) = \exp(-r)(15 + 15r + 6r^2) \in C^6$

We expect the RBFs of lower continuity to be more suitable for approximating a signal characterized by steep gradients, as the MPI signal. We also point out that the Fake Nodes approach with RBFs shows strong similarities with the use of the so-called variably scaled (discontinuous) kernels, refer to [7], [14].

D. Performance evaluation

We evaluate the performance of each approach by comparing each reconstructed image A with the original image I (both made of K voxels) using the following criteria:

- 1) Relative 1-norm error (the smaller the better)

$$\text{err1}(A, I) = \frac{\sum_{i=1}^K |A_i - I_i|}{\sum_{i=1}^K |I_i|}.$$

- 2) Symmetrized Kullbak-Leibner Divergence (the smaller the better)

$$\text{SKL}(A, I) = \text{KL}(A, I) + \text{KL}(I, A),$$

where the Kullbak-Leibner Divergence is defined as

$$\text{KL}(v, w) = \frac{\sum_{i=1}^K w_i \log\left(\frac{v_i}{w_i}\right)}{K}.$$

- 3) The Structural SIMilarity index (or **SSIM**, the larger the better)

$$\text{SSIM}(A, I) = \frac{(2\bar{A}\bar{I} + c_1)(2\Sigma_{AI} + c_2)}{(\bar{A}^2 + \bar{I}^2 + c_1)(\Sigma_A^2 + \Sigma_I^2 + c_2)} \in [0, 1]$$

where \bar{A} denotes the mean and Σ_A the standard deviation, and $c_1, c_2 \in \mathbb{R}$ two default-chosen numbers used to stabilize the formula.

These three measures will be evaluated both for standard and Fake Nodes approximations to show the difference. Computations are all performed in the cloud via MATLAB Online webpage: matlab.mathworks.com.

V. RESULTS

The resulting accuracy indicators for each image reconstruction method are shown in Table I. For both polynomials and RBFs the introduction of the Fake Nodes leads to a better reconstruction according to all the considered metrics, except for the case of RBF φ_2 , where curiously the SKL increases when using the Fake Nodes.

It has to be noticed that RBF methods using basis functions with low regularities slightly outperform polynomial reconstruction both with and without the usage of the Fake Nodes in all metrics except for SKL. As can be observed in Figure 2, the polynomial approximation tends to smooth out the image with respect to RBF interpolation methods, which however tend to include some of the noise generated in synthesis.

	err1	SKL	SSIM
Polynomial	1.6763	1.3581	0.2191
Fake-Polynomial	1.1541	0.6424	0.5546
RBF φ_0	1.1120	0.7369	0.6843
Fake-RBF φ_0	1.1078	0.6833	0.7091
RBF φ_2	1.0995	0.7947	0.6759
Fake-RBF φ_2	1.0689	0.8117	0.7135
RBF φ_4	1.1036	0.8050	0.6651
Fake-RBF φ_4	1.0686	0.9137	0.7110
RBF φ_6	1.4674	1.0779	0.1571
Fake-RBF φ_6	1.2159	1.0154	0.4152

TABLE I
PERFORMANCES OF EACH METHOD IN THREE METRICS.

VI. DISCUSSION AND FUTURE WORKS

We presented an effective method for the reconstruction of MPI images based on the so-called Fake Nodes. In doing so we also compared the accuracy of two different reconstruction tools, i.e. polynomial least squares and kernel-based interpolation. In their standard form both methods suffer from Gibbs artifacts, while when using the Fake Nodes such oscillations are mitigated for both bases. The results show that the two methods are comparable for this bio-imaging application, even if the kernel-based interpolation via Fake

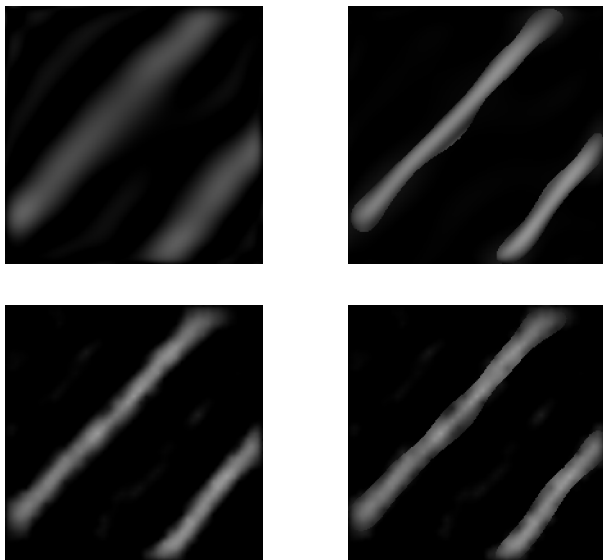


Fig. 2. Top left: reconstructed image by means of polynomial least-squares on the original data. Top right: reconstruction with polynomial least-squares on Fake Nodes. Bottom left: reconstruction with RBF with φ_0 on original data. Bottom right: reconstruction with RBF (with φ_0) on Fake Nodes.

Nodes slightly outperforms the approximation obtained via polynomial least squares, provided that the regularity of the kernel is small enough. In fact increasing the regularity of the basis function leads in our experiments to slightly better results in terms of err1 and SSIM until the Matérn C^6 , while on the other side the error in terms of SKL seems to get higher progressively as the regularity increases. This seems to indicate a greater sensitivity of SKL measure in measuring errors in this kind of images, indicating φ_0 as the best basis function between the ones that are tested.

The advantage of the Fake Nodes approach based on kernels is that the so-constructed basis, being data-dependent, allows us to interpolate at the nodes. On the opposite with the polynomial basis, we have to relax the interpolation conditions and perform a least square approximation. This might lead, as in our case, to a decrease of the accuracy in the reconstruction, due to the excessive smoothing effect. However, the polynomial least squares approximation is suggested when the number of nodes grows. Indeed, to interpolate with RBFs, we need to solve a linear system whose system matrix belongs to $\mathbb{R}^{(N+1) \times (N+1)}$. In the considered examples, the polynomial Vandermonde matrix has a smaller size. Precisely it belongs to $\mathbb{R}^{(N+1) \times (M+1)}$, and if $M \ll N$, this surely leads to a saving in terms of memory needs. In view of these considerations, work in progress consists in investigating the Fake Nodes scheme in the context of other bio-medical applications such as image denoising [8], resolution approximation of an imaging system [9] and MEG/EEG reconstruction [1], [2]. Moreover we intend to investigate the use of Fake Nodes interpolation in clinical imaging studies [19] and how the kernel Moving Least Squares (see e.g. [18], [21]) performs for MPI images.

ACKNOWLEDGMENTS

This research has been accomplished within Rete Italiana di Approssimazione (RITA), partially funded by GNCS-INδAM and through the European Union's Horizon 2020 research and innovation programme ERA-PLANET, grant agreement no. 689443, via the GEOEssential project.

REFERENCES

- [1] G. ALA, E. FRANCOMANO, G. E. FASSHAUER, S. GANCI, M. J. MCCOURT, *A Meshfree Solver for the MEG Forward Problem*, IEEE Transactions on Magnetics, **51:3** (2015), 1–4.
- [2] G. ALA, G. E. FASSHAUER, E. FRANCOMANO, S. GANCI, M. J. MCCOURT, *The method of fundamental solutions in solving coupled boundary value problems for M/EEG*, SIAM Journal on Scientific Computing, SIAM Journal on Scientific Computing **37:4** (2015), B570–B590.
- [3] R. ARCHIBALD, A. GELB, J. YOON, *Fitting for edge detection in irregularly sampled signals and images*, SIAM J. Numer. Anal. **43** (2005), 259–279.
- [4] A. BAYLISS, E. TURKEL, *Mappings and accuracy for Chebyshev pseudo-spectral approximations*, J. Comput. Phys. **101** (1992), 349–359.
- [5] L. BOS, M. CALIARI, S. DE MARCHI, M. VIANELLO AND Y. XU, *Bivariate Lagrange interpolation at the Padua points: the generating curve approach*. J. Approx. Theory **143** (2006), 15–25.
- [6] L. BOS, S. DE MARCHI, M. VIANELLO, *Polynomial approximation on Lissajous curves in the d-cube*. Appl. Numer. Math. **116** (2017), pp. 47–56.
- [7] M. BOZZINI, L. LENARDUZZI, M. ROSSINI, R. SCHABACK, *Interpolation with variably scaled kernels*, IMA J. Numer. Anal. **35** (2015), 199–219.
- [8] R. CAMPAGNA, S. CRISCI, S. CUOMO, L. MARCELLINO, G. TORALDO, *Modification of TV-ROF denoising model based on Split Bregman iterations*, Appl. Math. Comput. **315** (2017), pp. 453–467.
- [9] D. CECCHIN, D. POGGIALI, L. RICCARDI, P. TURCO, F. BUI, S. DE MARCHI, *Analytical and experimental FWHM of a gamma camera: theoretical and practical issues*, PeerJ **2**, e722 (2015), doi: 10.7717/peerj.722.
- [10] P.J. DAVIS, *Interpolation and Approximation*, Dover Publications, 1975.
- [11] S. DE MARCHI, W. ERB, F. MARCHETTI, *Spectral filtering for the reduction of the Gibbs phenomenon for polynomial approximation methods on Lissajous curves with applications in MPI*, Dolomites Res. Notes Approx. **10** (2017), pp. 128–137.
- [12] S. DE MARCHI, W. ERB, F. MARCHETTI, *Lissajous sampling and spectral filtering in MPI applications: the reconstruction algorithm for reducing the Gibbs phenomenon*, 2017 International Conference on Sampling Theory and Applications (SampTA), Tallin (2017), pp. 580–584.
- [13] S. DE MARCHI, W. ERB, F. MARCHETTI, E. PERRACCHIONE, M. ROSSINI, *Shape-Driven Interpolation with Discontinuous Kernels: Error Analysis, Edge Extraction and Applications in MPI*, to appear on SIAM Sci. Comput. 2020, DOI: 10.1137/19M1248777.
- [14] S. DE MARCHI, F. MARCHETTI, E. PERRACCHIONE, *Jumping with Variably Scaled Discontinuous Kernels (VSDKs)*, to appear on BIT Numerical Mathematics, 2019, doi: 10.1007/s10543-019-00786-z, 2019.
- [15] S. DE MARCHI, F. MARCHETTI, E. PERRACCHIONE, D. POGGIALI, *Polynomial interpolation via mapped bases without resampling*, J. Comput. Appl. Math., **364** (2020), 112347–12.
- [16] W. ERB, *Bivariate Lagrange interpolation at the node points of Lissajous curves - the degenerate case*, Appl. Math. Comput. **289** (2016), 409–425.
- [17] W. ERB W. C. KAETHNER, M. AHLBORG AND T.M. BUZUG *Bivariate Lagrange interpolation at the node points of non-degenerate Lissajous nodes*, Numerische Mathematik **133:4** (2016), 685–705,
- [18] G. FASSHAUER, *Meshfree Approximation Methods with MATLAB*, World Scientific Publishing Co., Singapore, 2007.
- [19] A. FAVARETTO, A. LAZZAROTTO, D. POGGIALI, G. ROLMA, F. CAUSIN, F. RINALDI, P. PERINI, P. GALLO, *MRI-detectable cortical lesions in the cerebellum and their clinical relevance in multiple sclerosis*, Mult. Scler. **22** (2016), pp. 494–501.

- [20] B. FORNBERG, N. FLYER, *The Gibbs Phenomenon in Various Representations and Applications*, chapter The Gibbs phenomenon for radial basis functions. Sampling Publishing, Potsdam, NY, 2008.
- [21] E. FRANCOMANO, F.M. HILKER, M. PALIAGA, E. VENTURINO, *An efficient method to reconstruct invariant manifolds of saddle points*, Dolomites Res. Notes Approx. **10** (2017), pp. 25–30.
- [22] C. KAETHNER, W. ERB, M. AHLBORG, P. SZWARGULSKI, T. KNOPP, AND T.M. BUZUG *Non-Equispaced System Matrix Acquisition for Magnetic Particle Imaging based on Lissajous Node Points*. IEEE Transactions on Medical Imaging, **35**,11 (2016), pp. 2476–2485.
- [23] T. KNOPP AND T.M. BUZUG *Magnetic Particle Imaging*. Springer, 2012.
- [24] L. ROMANI, M. ROSSINI, D. SCHENONE, *Edge detection methods based on RBF interpolation*, J. Comput. Appl. Math. **349** (2019), 532–547.
- [25] M. ROSSINI, *Interpolating functions with gradient discontinuities via variably scaled kernels*, Dolom. Res. Notes Approx. **11** (2018), 3–14.